Application of Production Data Integration by Numerical Calculation of Sensitivity Coefficients

Linan Zhang[1], Thies Dose[2], Clayton V. Deutsch[1], and Luciane Cunha[1]

[1]Civil & Environmental Engineering
University of Alberta

[2]RWE-DEA Aktiengesellschaft

Abstract

This paper is the second in a three-part series that presents a practical methodology for production data integration in large reservoirs with long production/injection history. The focus of this paper is the application of the methodology to a reservoir with realistically complex geologic structure and production history. The details of the field are not fully disclosed because they are not necessary; the main point of the paper is to demonstrate the practical applicability of the methodology.

Introduction

A new methodology that can integrate well bottom hole pressure and fractional flow rate into large reservoir models by the numerical calculation of sensitivity coefficients was proposed in the preceding paper. This paper shows the application to a reservoir with 9 active wells, where 3 wells were converted into injectors, two wells were shut-in and there are four new wells.

ECLIPSE was used for simulation. There are 235,800 grid blocks in the property models. The liquid production rate and water injection rate are input parameters in the flow simulation model. The pressure and the quarterly averaged oil production rate are the parameters to match. The permeability models were updated. The porosity model was fixed

Two base realizations with different means are considered (Model A and Model B). The horizontal permeabilities in the X and Y directions are set to be the same. The horizontal permeability in the X direction is highly correlated to the permeability in the Z direction with a correlation coefficient of 0.901. Therefore, one factor was used to perturb all three permeability models. Two well schedule files with different well production index settings were considered (Schedule A and Schedule B – unrelated to Model A/B).

Since there are only 9 active wells in the reservoir, only one perturbation location per iteration was selected. The use of one perturbation location worked for this problem. The general principle is to select the perturbation locations at the locations with high mismatch.

The weights for pressure and fractional flow rate were thought to be same so that $w_p = w_q = 1$. The weight for mismatch at the well with index w, β_w, was obtained from the ratio of the total working time of the well of interest over the sum of the working time of all wells. In the processing, the working time for producers is their production time but for the wells that were producers at first and then were converted into injectors working time is the sum of production time and injection time.

Weights for the observed rates at each well, $\lambda_{w,q,t}$, can be set to any values based on the importance of the data. In the application, all the historical oil production rates were equally weighted.

Weights for well bottom-hole pressure data, $\lambda_{w,p,t}$, can be set to any values based on the importance of the data. In our application, the weights were set to the ratio of "effective time" of each observed datum against the total "effective" time of all data at that well. This gives low weights to the closely spaced redundant data.

The reservoir is water-wet, stratified and the simulation is liquid rate controlled; therefore, in general, an increase in permeability around a producer tends to increase the water production rate and decrease the oil production rate at the well. This was used to select the perturbations and to accelerate convergence.

Results of the Application

In this part, the methodology with only one perturbation location was applied to the two different base iterations with the two different schedule files. Change of the global mismatch of reservoir with iterations, change of the global mismatch at each well with iterations and effect of multipliers of pore volume and permeability were studied.

Change of Global Mismatch of Reservoir with Iterations

The methodology was used to update Model A with Schedule A. One perturbation location was selected in each iteration, as shown in Figure 1. The perturbations were propagated to the entire grid system with a spherical type of variogram and a range of 4 grid blocks for iterations 1 to 5 and 3 grid blocks (about half well space) for iteration 6 to 8. The global mismatch values are shown in Figure 2. The mismatch decreases with iterations. After the eighth iteration, the mismatch in oil production rates of the updated model decreased by 80% from the initial model, the mismatch in pressure decreased by 8%.

This methodology was applied to model B with the same schedule. The perturbation locations are shown in Figure 3. The results of mismatch change with iterations are shown in Figure 4. The mismatch in the fractional flow rate decreased by about 80%. The pressure mismatch decreased by about 16%.

Effect of Base Model and Schedule File

The methodology was applied to two sets of property models and schedule files. The results in Figure 5 show that the proposed methodology can be used to build property models corresponding to a similar global mismatch. The global mismatch with different schedule files converge to different mismatch levels. Setting appropriate well conditions is important. The changes in the area between the wells are consistent between multiple realizations, as shown in Figure 6.

Change of Global Mismatch at Each Well with Iterations

It is difficult to improve the mismatch at all wells and all times at every iteration. This can be seen by comparing global mismatch at each well, as shown in Table 1. Some changes at the perturbation locations may make some wells match better but make others match worse. This is because increasing permeability around a producer tends to increase the water rate at the well but decrease water rate at adjacent wells that are connected to the same injector because the water injection rate at the injector is fixed in the ECLIPSE model.

It can be seen from Table 1 that the mismatch in oil production rates at all wells for the updated model are smaller than the base model except Well 3. The match in pressure for the updated models at wells 2, 5, 8 and 9 are worse than the base model. The global mismatch at Wells 3 and 9 in the updated model are worse than those of the base model. We did not set perturbation locations near Wells 2 and 3 so that the changes of production behaviors of the wells are small no matter how the property at the perturbation location changes. In addition, Wells 6 and 7 only produced oil for a short period and were shut-in permanently. Wells 8 and 9 were producers at the beginning of the development and are injectors now. Well 5 is a new producer. The well production indexes and skin factors have a large effect on the well bottom-hole pressure. Wells 5, 8 and 9 experienced stimulation work but their well production indexes were set as constant in Schedule file A; updating those values would improve the match (see below)

The curves of pressure and oil production rates at the four wells are shown in Figures 7. The mismatch in oil production rates and pressure at Well 1 are improved and can be seen from the figures. Well 4 is a new producer and the mismatch in oil production rates and pressure at the well are improved but it is hard to see the improvement of pressure mismatch from the figures. Well 6 is an old producer and the mismatch in oil production rates at the well is improved but the pressure observation is too few so that we are not sure about the improvement of the pressure mismatch. Well 9 got an almost perfect match in oil production rates but a worse match in pressure between observed data and simulation results.

Effect of Well Production Index on Mismatch in Pressure at Wells

The well production index (WPI) is a parameter that has a large effect on simulated well performance. Considering that well production index at Well 9 may be changed around time of 6100 and the historical pressure is higher than the simulation results of the updated model after that time, the changing of well production index at Well 9 from 3.0 to 2.5 in the Schedule A made the mismatch in pressure at the well be improved much, shown in Figure 8. The well production index has little effect on mismatch in oil production rates.

Effect of Multipliers of Pore Volume and Permeability

The combination of the updated property model B with schedule A was used in a sensitivity study on the multiplier of pore volume. The results are shown in Figure 9, which shows that multiplier of pore volume of 1 used in the current Eclipse model, is a good choice with respect to the lowest global mismatch. It is interesting to see that the mismatch in pressure decreases with the increase of pore volume multiplier in the considered range. The multiplier of pore volume has a larger effect on rate mismatch than on pressure mismatch.

The combination of the updated property model B with the schedule file A was used in the sensitivity study on the multiplier of horizontal permeability. The results are shown in Figure 10, which shows that the current choice is reasonable. The multiplier of horizontal permeability has a larger effect on pressure mismatch than on rate mismatch.

The change of mismatch of the reservoir with the multipliers of pore volume and horizontal permeability between the original model B and the updated model B with Schedule A are shown in Figures 11 and 12. From Figures 11 and 12, we can see that the multiplier of pore volume has a larger effect on rate mismatch than on pressure mismatch. From Figures 11 and 12, it also can be seen that the multipliers of pore volume and horizontal permeability corresponding to the lowest global mismatch for the base model are a little different from those for the updated model, shown in Table 2. The global mismatch of the updated model with the multiplier of horizontal permeability of 2.5 is 36.9%, which is just a little higher that the value of 36.3% in the case that multiplier of horizontal permeability of 2.9 is used. Multiplier of horizontal permeability between 2.5 to 3.5 seems to be good for the updated model. The inversion method leads to multipliers that give a low global mismatch.

The comparison of the results by applying the proposed methodology to Model B with Schedule B with current multipliers and optimal multipliers is shown in Figure 13. One perturbation location was selected at each iteration based on the largest product of global mismatch and oil rate mismatch. The spherical variogram was selected as the perturbation variogram and the perturbation range was set as 4 grid blocks. Figure 13 shows that optimal multipliers dramatically improve convergence in the first few iterations. Good multipliers can take fewer iterations to get an acceptable mismatch level.

Change of Global Mismatch with Iterations in case of Multiple Perturbations at each Iteration

For the sake of efficiency, multiple perturbation locations were selected in each iteration when applying the methodology to base Model B with Schedule B. The exponent ω in the pressure and oil production rates decomposition equations is set to 1. The perturbations were propagated to the entire grid system by simple kriging with range 3 grid block sizes and variogram of Gaussian type. The mismatch for the updated model after sixth iterations reached the level for the updated model after 10^{th} iterations in case of one perturbation location in each iteration. The perturbation locations are shown in Table 3.

The results of mismatch change with iterations are shown in Figure 14. It can be seen that the global mismatch of the reservoir and mismatch in fractional flow rates decrease with iterations. The comparison of the global mismatch after application of the methodology with one perturbation location and that with multiple perturbation locations is shown in Figure 15, which shows that the use of multiple perturbation locations makes the methodology require less iterations than one perturbation in each iteration to get similar mismatch levels.

Figure 16 shows the comparison of the permeability map in the top layer of the updated model after application of the methodology with one perturbation location and that with multiple perturbation locations. The two maps are very similar.

Conclusions

This method makes it possible to condition permeability/porosity realizations to production rates and pressure historical data. This application demonstrates that the proposed methodology is efficient and practical for large reservoir models. The global mismatch of the reservoir corresponding to the updated models decreases with iteration. In this case, the fractional rate was matched better than pressure. The proposed method can post-process realizations to similar low levels. The well settings are very important to the calculated pressure values. We could imagine changing other well control parameters to improve the pressure match.

The use of multiple perturbation locations makes the methodology more efficient but does not change the final results much from that with one perturbation location in each iteration. The entire procedure was run in a *manual* mode to permit greater understanding and sensitivity analysis; however, it could be fully automated with a script. A fully automatic scheme would be essential for processing many realizations.

Item	Iteration	Well 1	Well 2	Well 3	Well 4	Well 5	Well 6	Well 7	Well 8	Well 9
Pressure Mismatch ΔP_w^i	0	2985	807	1505	10203	315	578	114	367	1616
	1	2046	872	1488	9308	330	598	67	404	2187
	2	1713	924	1483	9050	348	646	58	466	2640
	3	1718	913	1485	9126	346	418	50	487	2742
	4	1724	916	1487	7627	350	412	54	524	2840
	5	1741	909	1493	7658	348	387	93	496	2809
	6	1744	904	1493	7677	347	359	96	501	2858
	7	1747	904	1494	7250	349	357	97	510	2886
	8	1756	897	1496	7243	347	341	61	507	2716
		better	worse	better	better	worse	better	better	worse	worse
Rate Mismatch ΔQ_w^i	0	265.4	47.7	35.1	867.1	7.0	74.1	1.1	162.2	0.002
	1	106.5	42.0	46.9	625.0	2.5	132.6	0.6	159.3	0.001
	2	20.4	34.7	55.6	669.4	1.3	190.7	0.5	121.8	0.001
	3	26.9	35.5	57.1	707.1	0.9	105.7	0.5	92.6	0.001
	4	26.91	39.32	62.23	213.2	0.77	105.5	0.46	92.25	0.001
	5	13.8	38.0	60.6	233.8	1.0	65.6	0.8	44.2	0.001
	6	16.1	38.5	61.1	248.8	0.8	31.4	0.7	47.2	0.001
	7	16.1	33.0	78.2	124.9	2.3	31.4	0.7	47.5	0.001
	8	24.6	33.8	77.5	110.8	2.2	27.2	0.4	37.0	0.001
		better	better	worse	better	better	better	better	better	better
Global Mismatch Δ_w^i	0	0.275	0.019	0.022	0.143	0.003	0.042	0.000	0.107	0.067
	1	0.146	0.019	0.024	0.116	0.002	0.064	0.000	0.107	0.090
	2	0.083	0.018	0.025	0.118	0.002	0.086	0.000	0.088	0.109
	3	0.087	0.018	0.025	0.122	0.002	0.049	0.000	0.073	0.113
	4	0.088	0.019	0.026	0.069	0.002	0.049	0.000	0.074	0.117
	5	0.081	0.019	0.026	0.071	0.002	0.034	0.000	0.046	0.116
	6	0.082	0.019	0.026	0.072	0.002	0.021	0.000	0.048	0.118
	7	0.082	0.018	0.028	0.059	0.003	0.021	0.000	0.048	0.119
	8	0.088	0.018	0.028	0.057	0.003	0.019	0.000	0.042	0.112
		better	better	worse	better	fixed	better	fixed	better	worse

Table 1. Pressure and oil rate mismatch at each well for base Model A with Schedule A.

	Multiplier of Pore Volume	Multiplier of Horizontal Permeability
Used in the Model	1.0	2.5
Best for the base Model B (range for low mismatch)	0.9 (0.875 to 0.95)	3.5 (3 to 4)
Best for the Updated Model (range for low mismatch)	1.0 (0.95 to 1)	2.9 (2.5 to 3.5)

Table 2. Multipliers used in the Eclipse Model and the best values for Model B and the updated Model B (multiplier of pore volume=1.0).

Iteration	Perturbation locations
1st	Locations at Wells 1,3,4,6 and 8
2nd	Locations at Wells 1,3 and 4
3rd	Locations at Wells 1,3 and 4
4th	Locations at Wells 1 and 4
5th	Location at Wells 1
6th	Locations at Wells 1,3,4 and 6

Table 3. The perturbation locations in each iteration.

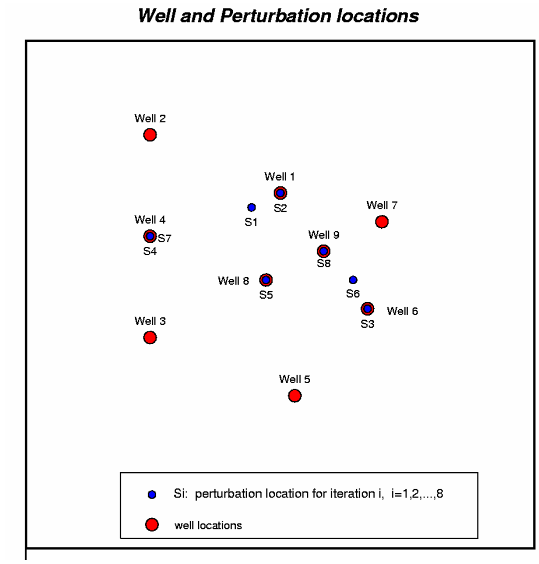

Figure 1. Perturbation locations in application of the methodology to Model A with Schedule A.

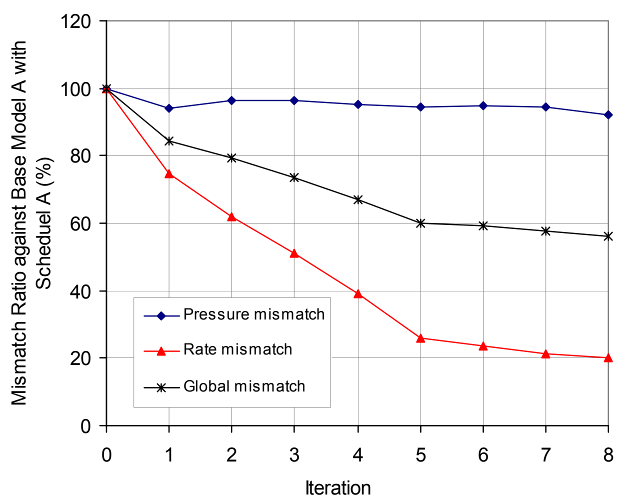

Figure 2. Mismatch with iterations for Model A with Schedule A.

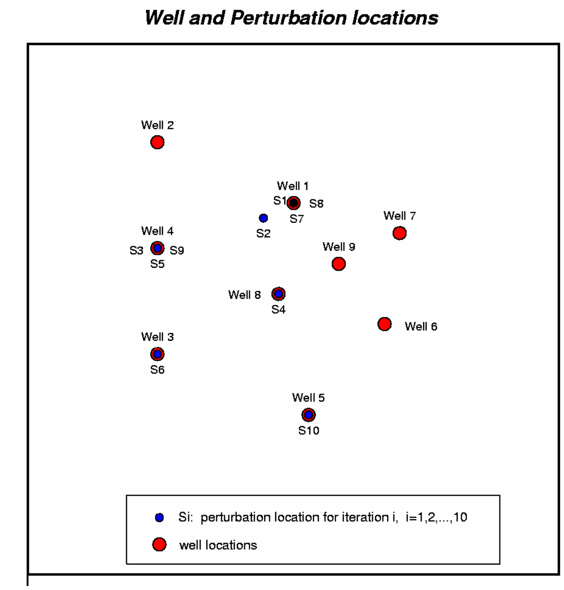

Figure 3. Perturbation locations in application of the methodology to Model B with Schedule B.

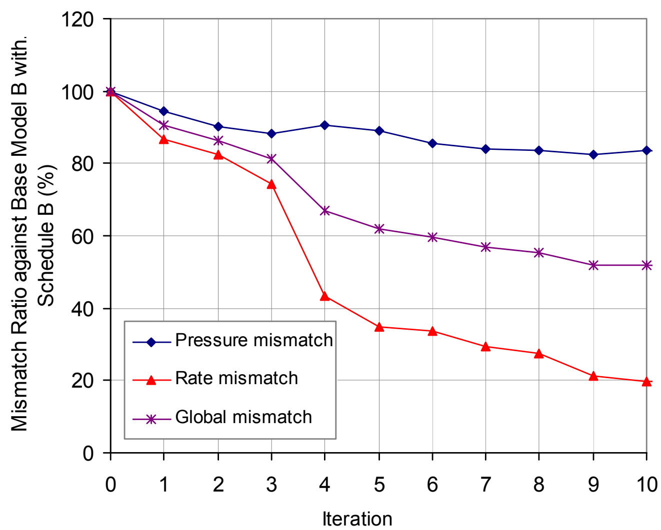

Figure 4. Mismatch with iterations for Model B with Schedule B.

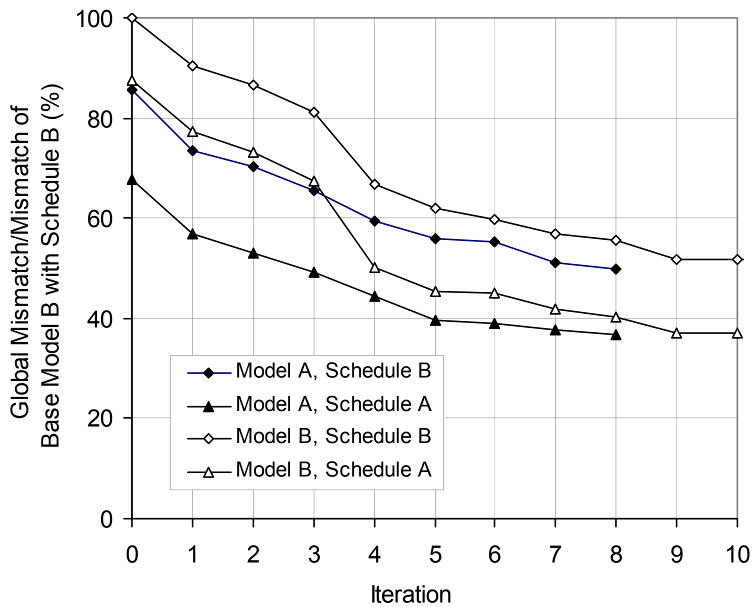

Figure 5. Global mismatch of updated models started from the different combinations of property models and schedule files.

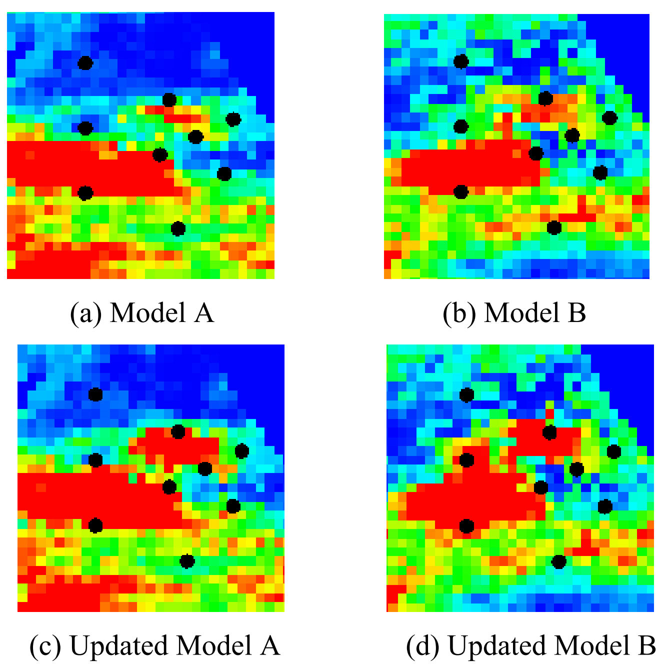

Figure 6. Maps of permeability in the X direction in the top layer for the two base models and their updated models.

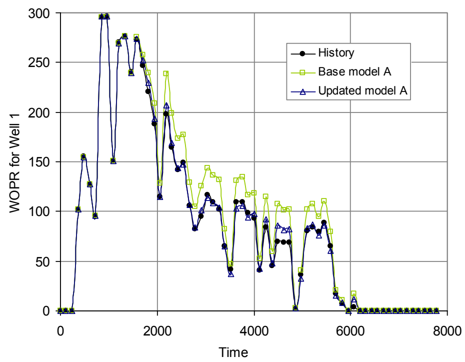
WOPR for Well 1
Time
History
Base model A
Updated model A

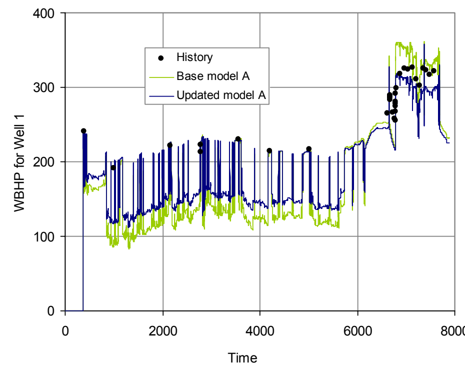
WBHP for Well 1
Time
History
Base model A
Updated model A

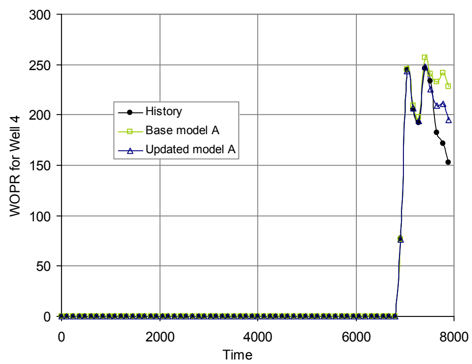
WOPR for Well 4
Time
History
Base model A
Updated model A

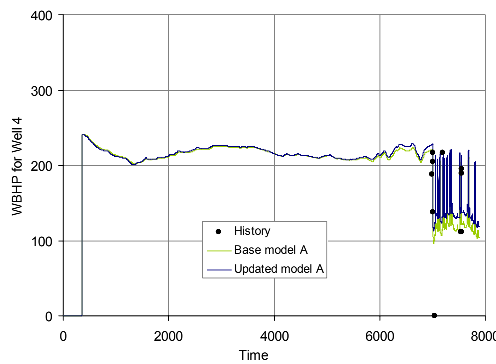
WBHP for Well 4
Time
History
Base model A
Updated model A

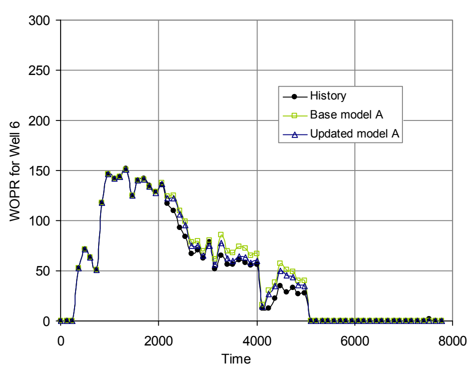
WOPR for Well 6
Time
History
Base model A
Updated model A

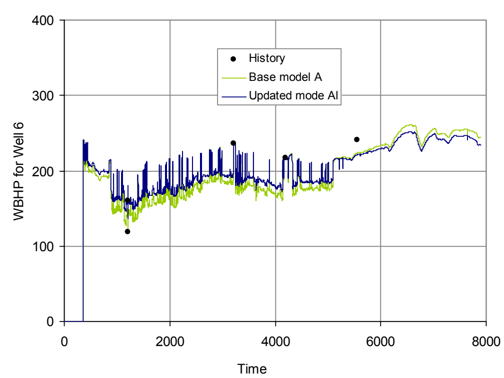
WBHP for Well 6
Time
History
Base model A
Updated mode Al

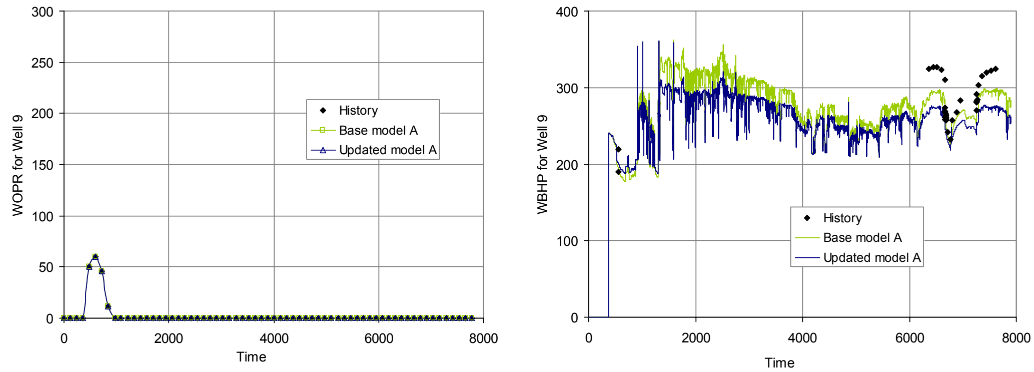

Figure 7. The curves of oil production rates and well bottom-hole pressure at the four wells for Model A and updated Model A with Schedule A.

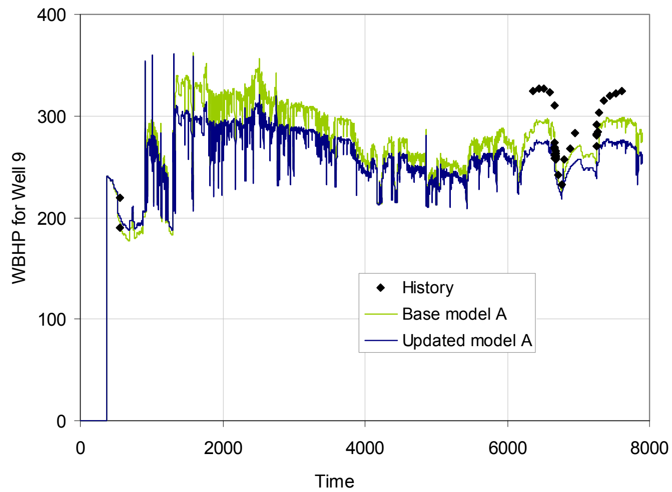

(a) Original schedule

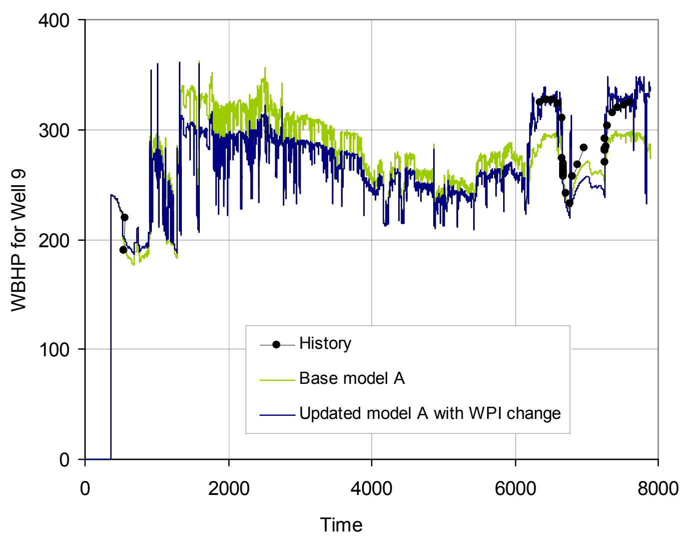

(b) the updated schedule by changing WPI at well 9
from 3 to 2.5 after time of 6100

Figure 8. Effect of well production index (WPI) on history match.

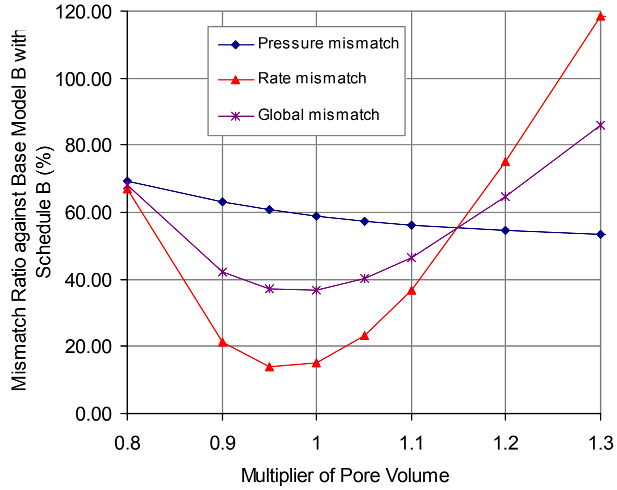

Figure 9. Mismatch with different multipliers of pore volume.

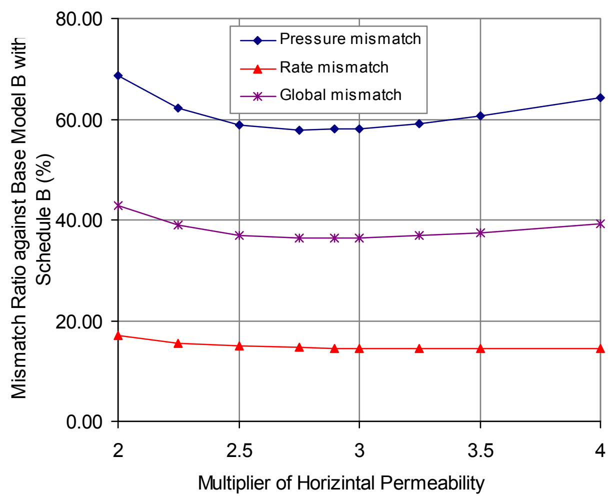

Figure 10. Mismatch with different multipliers of permeability.

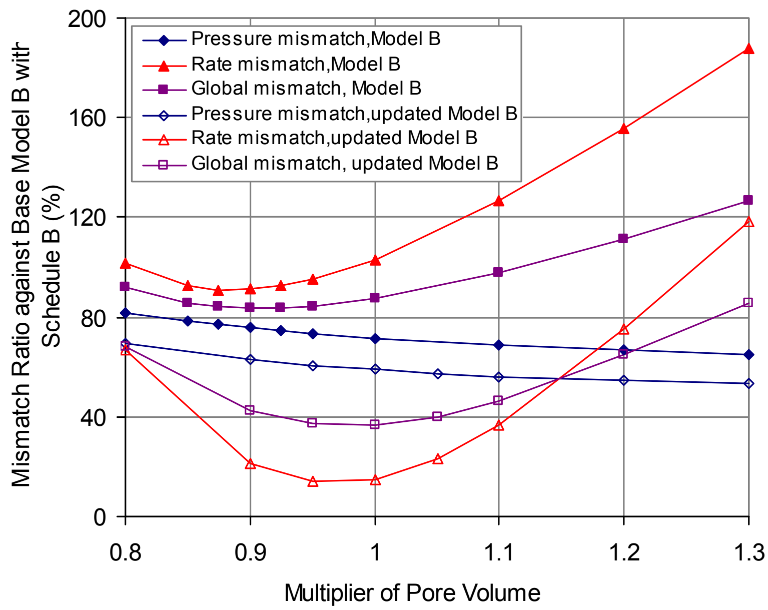

Figure 11. Comparison of mismatches from Model B and updated model B coupled with Schedule A at different multipliers of pore volume (multiplier of horizontal permeability=2.5).

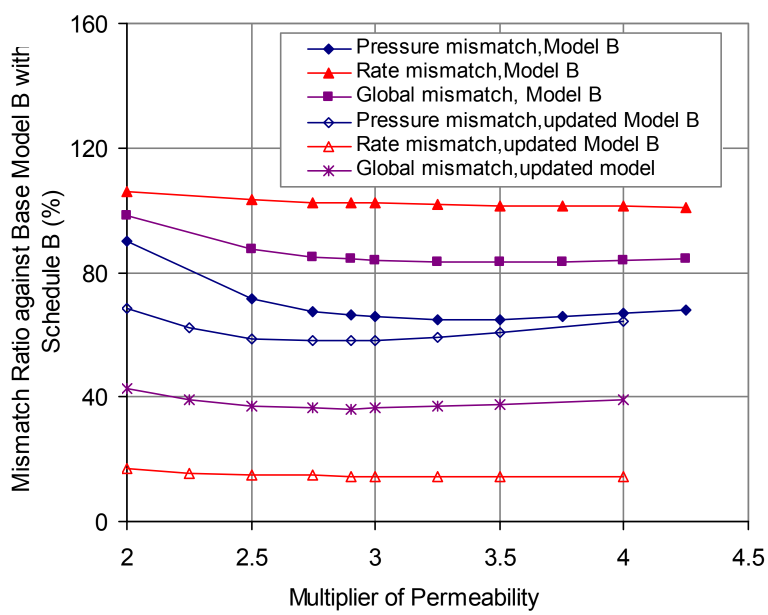

Figure 12. Comparison of mismatches from Model B and updated model B with Schedule A at different multipliers of horizontal permeability (multiplier of pore volume=1.0).

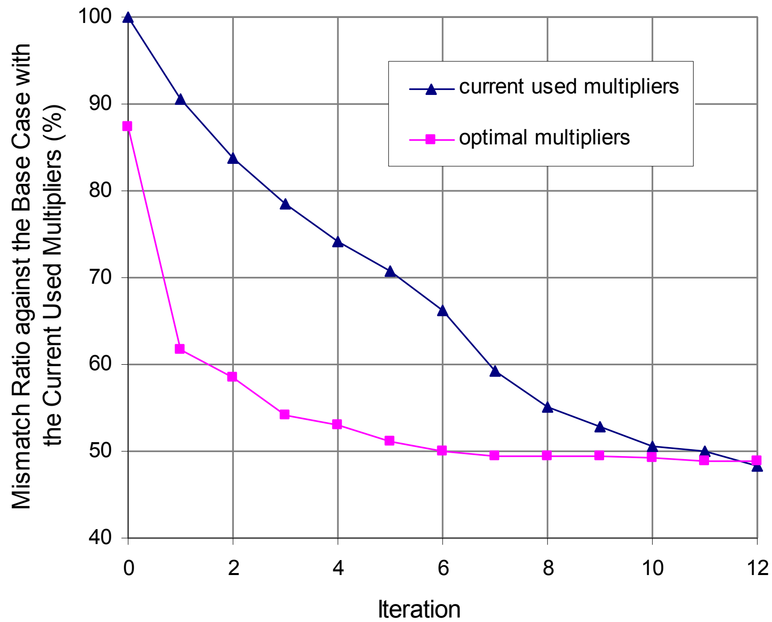

Figure 13. Comparison of global mismatch between the updated models for different multipliers of permeability and pore volume

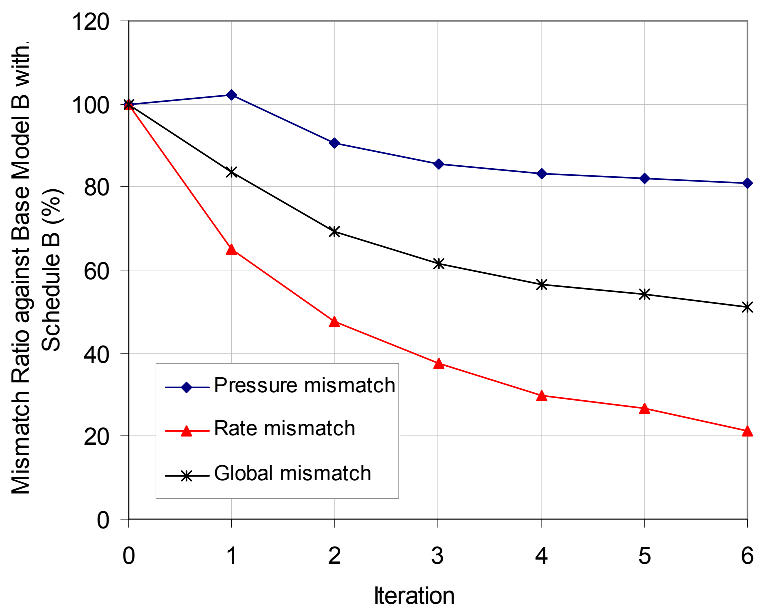

Figure 14. Mismatch with iteration for Model B after applying the methodology with multiple perturbation locations for each iteration.

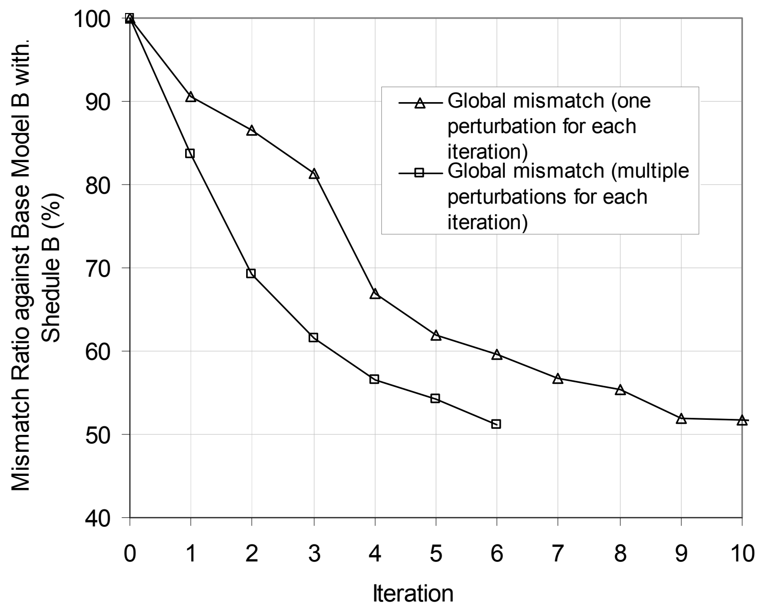

Figure 15. The comparison of application of the methodology with one perturbation location and that with multiple perturbation locations.

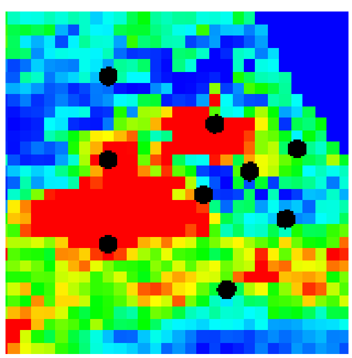

(a) Updated model B after the 10th iteration with one perturbation in each iteration

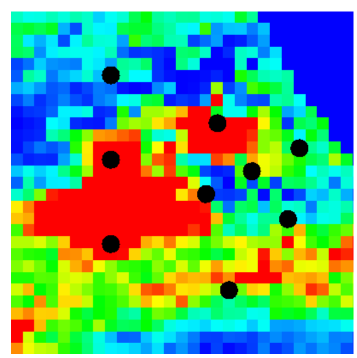

(b) Updated model B after the 6th iteration with multiple perturbations in each iteration

Figure 16. The comparison of application of the methodology with one perturbation location and that with multiple perturbation locations.